

Computational Analysis on Calcium Dynamics of Vascular Endothelial Cell Modulated by Physiological Shear Stress

Hyun Goo Kang¹, Eun Seok Lee¹, Eun Bo Shim² and Keun Shik Chnag^{1¶}

¹ Division of Aerospace engineering, Department of Mechanical Engineering, Korea Advanced Institute of Science and Technology

² Department of Mechanical & Biomedical Engineering, Kangwon National University

Abstract

Flow-induced dilation of blood vessel is the result of a series of bioreaction in vascular endothelial cells(VEC). Shear stress change by blood flow in human artery or vein is sensed by the mechanoreceptor and responsible for such a chain reaction. The inositol(1,4,5)-triphosphate(IP_3) is produced in the first stage to elevate permeability of the intercellular membrane to calcium ions by which the cytosolic calcium concentration is consequently increased. This intracellular calcium transient triggers synthesis of EDRF and prostacyclin. The mathematical model of this VEC calcium dynamics is reproduced from the literature. We then use the Computational Fluid Dynamics(CFD) technique to investigate the blood stream dictating the VEC calcium dynamics. The pulsatile blood flow in a stenosed blood vessel is considered here as a part of study on thrombogenesis. We calculate the pulsating shear stress (thus its temporal change) distributed over the stenosed artery that is implemented to the VEC calcium dynamics model. It has been found that the pulsatile shear stress induces larger intracellular Ca^{2+} transient plus much higher amount of EDRF and prostacyclin release in comparison with the steady shear stress case. It is concluded that pulsatility of the physiological shear stress is important to keep the vasodilation function in the stenosed part of the blood vessel. Key words: Atherosclerosis, Computational Fluid Dynamics, Medical Imaging.

Introduction

Vascular Endothelial cells lining the inner surface of the blood vessel are continuously exposed to shear stress due to the blood stream. Flow-induced dilation of blood vessel is associated with endothelial calcium dynamics and response of smooth muscle cells in the tunica media sensing shear stress change in the blood flow. The inositol (1,4,5)-triphosphate(IP_3), produced in this shear stress-mediated chain reaction, controls permeability of the intracellular membrane to the calcium ions that works as a mediator or the second messenger of endothelium-derived vasodilation.

Much studies have been made on the shear stress-calcium reaction mechanism inside the vascular

endothelial cells(VEC). Ando *et al.*¹ reported that Ca^{2+} concentration is transient in the cultured VEC as it was exposed to a flow stream. Nollert *et al.*² found that the fluid shear stress induces production of inositol (1,4,5)-triphosphate(IP_3) and it led to the release of Ca^{2+} from the intracellular calcium ion store. Shen *et al.*³ performed in-vitro experiment with the cultured bovine aortic endothelial cells by exposing them to laminar shear stress in a parallel-plate flow chamber. They found that shear stress triggered IP_3 -pathway resulting in Ca^{2+} response inside the VEC. Ando *et al.*⁴ further demonstrated that the mechanical deformation of VEC due to the wall shear stress initiated the flow-induced Ca^{2+} response. On the other hand, Olsen *et al.*⁵ and Kuo *et al.*⁶ found that some mechanoreceptor reduced transmembrane K^+ flux in response to the shear stress.

¶ 305-701 Guseong-dong, Yuseong-gu, Daejeon, Korea
kschang@kaist.ac.kr

These studies reveal that the VEC have not only the receptor to some agonist but also the mechanoreceptor which recognizes shear stress and induces Ca^{2+} response.

Based on these studies, Wong *et al.*^{7,8} proposed a vascular endothelial cell model which explained the mechanism of shear stress modulation of calcium dynamics and electrical activity. With this model, they performed various mathematical simulations to ascertain that the calcium dynamics and electrical activity of VEC was indeed modulated by the patterns of shear stress. In particular, by imposing a simple pulsatile shear stress it was shown that VEC was very sensitive to the rate of change of shear stress. Extending these fundamental results, we consider in this paper the more complicated patterns of VEC response to the physiological shear stress change in the human blood vessel.

Computational Fluid Dynamics(CFD) technique by which many engineers reliably calculate various external and internal flow phenomena are used to investigate the blood stream dictating the VEC calcium dynamics. The pulsatile blood flow in a stenosed blood vessel is considered with the study of thrombogenesis in mind. We first obtain the temporal change of fluctuating shear stress distributed over the stenosed artery. We then implement the VEC calcium dynamics model to look at the vascular dilation. In this way we are able to focus on the effect of shear stress on VEC when there is angiostenosis, which should be a very interesting topic to the general cardiovascular physiologists.

Materials and Methods

Blood flow in human artery and vein by periodic cardiac output causes temporal and spatial change in the distribution of fluid and wall shear stresses that affects the physiology of vascular endothelial cells. To investigate the effect of wall shear stress change on the calcium dynamics of VEC, we perform numerical simulation in two steps. First we simulate the pulsatile blood flow of human artery from which we obtain the spatial and temporal change of shear stress in the blood stream and on the endothelial wall. Second, we simulate the calcium dynamics and the consequent release of proteins or enzyme that initiates vasodilation of human artery and vein using the vascular endothelial cell model.

The cell model by Wong *et al.*^{7,8} describes how the shear stress modulates the cytosolic calcium concentration of human VEC and the release of endothelium-derived relaxing factor(EDRF) and prostacyclin(PGI_2). Fig. 1 schematically explains the model.

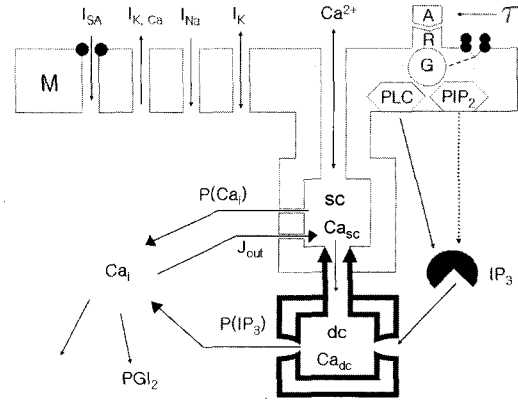


Fig 1. A two-compartment model for the vascular endothelial cells (from Wong *et al.*⁸).

Mechanoreceptor(mR) on the surface of VEC detects change in the wall shear stress(τ) that is induced by pulsatile blood flow. The deformation of mR activates a specific G-protein, resulting in the production of inositol (1,4,5)-triphosphate(IP_3). This IP_3 works as a second messenger which involves in the release of calcium ion and vasodilation-activating substance like EDRF or prostacyclin in the cytoplasm of VEC. The production of IP_3 changes the permeability($P[IP_3]$) of dc (the IP_3 -sensitive Ca^{2+} compartment), resulting in the release of Ca^{2+} into the cytosol. This transient increase of intracellular Ca^{2+} concentration(Ca_i) triggers release of Ca^{2+} from the sc (the Ca_i -sensitive Ca^{2+} compartment). This is called CICR mechanism(Ca^{2+} induced Ca^{2+} release). The initial transient Ca^{2+} activates $I_{K,Ca}$ that means Ca^{2+} -activated potassium current. This current induces hyperpolarization of the cell and influences the currents of sodium and potassium(I_{Na} , I_K). I_{Na} and I_K are governed by Goldman-Hodgkin-Katz constant field equation(GHK eqn.). These three kinds of ionic currents determine membrane potential of the cell.

On the other hand, this initial Ca^{2+} transient activates protein kinase C which phosphorylates specific G protein⁹, resulting in decrease of IP_3 production. This process is called as Ca_i -dependent inactivation (f). The rate of Ca^{2+} release from dc declines due to the reduced IP_3 concentration and dc [Ca^{2+}]. Along with Ca^{2+} efflux to the sc (J_{out}), Ca_i declines and $I_{K,Ca}$ and f are reduced. Consequently, the Ca_i and the membrane potential return to the resting level.

Mathematical description of the VEC model

The mathematical system describing the cell model is composed of 6 or 8 ordinary differential equations. The equations are solved sequentially one by one at each time step. Among them, the equations used in this study are introduced as follows.

1) Shear stress and mechanoreceptors:

$$\frac{d[R_\tau]}{dt} = k_1\phi(\tau)[R] - k_2[R_\tau]$$

$[R_\tau]$ is the fraction of mR that is deformed or altered by τ .

2) Generation of IP_3 :

$$\frac{d[IP_3]}{dt} = k_3(\tau)(1-f)\frac{d[R_\tau]}{dt} - k_4(\tau)[IP_3]$$

(1)

Here, f is Ca_i -dependent inactivation governed by the following equation.

$$\frac{df}{dt} = \frac{k_f\Delta Ca_i}{\Delta Ca_i + K_{f,m}} - k_g f \quad (2)$$

3) Calcium concentration in dc (Ca_{dc}):

$$V_{dc} \frac{dCa_{dc}}{dt} = P_{sd}(Ca_{sc} - Ca_{dc}) - P(IP_3)(Ca_{dc} - Ca_i) \quad (3)$$

where $P(IP_3)$ is the permeability of dc induced by IP_3 .

4) Cytosolic calcium concentration (Ca_i):

$$V_{cell} \frac{dCa_i}{dt} = P(IP_3)(Ca_{dc} - Ca_i) + P(Ca_i)(Ca_{sc} - Ca_i) - J_{out} \quad (4)$$

5) Release or synthesis of EDRF and prostacyclin (PGI_2):

$$\frac{d[EDRF]}{dt} = \alpha_1 Ca_i^4 - \beta_1 [EDRF] \quad (5)$$

$$\frac{d[PGI_2]}{dt} = \alpha_2 [IP_3]^4 Ca_i - \beta_2 [PGI_2] \quad (6)$$

More details of these equations, parameters and constants can be found in Wong *et al.*^{7,8}. We didn't include the equations for the electrical characteristics of VEC for ionic currents and membrane potentials in this study. It shall be considered in the future research.

Computational fluid dynamics

In the first step of simulation, we solve two-dimensional incompressible Navier-Stokes equations for the pulsatile flow in the human artery or vein. They consist of three equations.

The continuity equation:

$$\frac{\partial u}{\partial x} + \frac{\partial v}{\partial y} = 0 \quad (7)$$

The momentum equations in the x- and y-directions:

$$\rho \left(\frac{\partial u}{\partial t} + u \frac{\partial u}{\partial x} + v \frac{\partial u}{\partial y} \right) = -\frac{\partial p}{\partial x} + \frac{\mu}{\text{Re}} \left(\frac{\partial^2 u}{\partial x^2} + \frac{\partial^2 u}{\partial y^2} \right) \quad (8)$$

$$\rho \left(\frac{\partial v}{\partial t} + u \frac{\partial v}{\partial x} + v \frac{\partial v}{\partial y} \right) = -\frac{\partial p}{\partial y} + \frac{\mu}{\text{Re}} \left(\frac{\partial^2 v}{\partial x^2} + \frac{\partial^2 v}{\partial y^2} \right) \quad (9)$$

Galerkin finite element method is used to numerically integrate the above governing differential equations. For time integration, PISO (Pressure-Implicit Operator-Splitting) algorithm is used. PISO demands less sub-iteration which makes the computation faster. It shows good performance for the unsteady calculation like the present pulsatile blood flow.

In this study, we assume the blood vessel is solid and the blood is an incompressible and Newtonian fluid with constant temperature. The velocity of flow on the vascular wall is set to zero for a viscous flow.

Results

There are some assumptions regarding application of the present cell model. The permeability of Ca^{2+} compartments ($P[IP_3]$, $P(Ca_i)$) and Ca^{2+} efflux mechanism (J_{out}) should not be changed. In particular, for simplicity CICR mechanism is

ignored($P(Ca_i) = 0$). The extracellular calcium concentration, $Ca_0 = 2 \text{ mM}$ and the resting Ca^{2+} concentrations of the dc and sc have the same values as Ca_0 . The resting intracellular Ca^{2+} concentration, $Ca_{i,0} = 50 \text{ nM}$. V_{dc} (volume of dc) is set to be 0.1% of V_{cell} (cell volume). Finally, all the values of some parameters and constants are normalized to the cell volume of 1 l.

The equations describing model of VEC are solved with Euler's method that are widely used in the numerical analysis. In this method, the smaller the time step is, the better the numerical resolution is. In this study, time step is set to be 5 ms.

Effect of constant shear stress

For validation of the cell model, we reproduced a few cases of Wong *et al.*⁸ with the same condition. Constant shear stress is applied to the cell model. Fig. 2 shows intracellular Ca^{2+} concentration (Ca_i) and Ca^{2+} concentrations of the dc (Ca_{dc}). Here the shear stress stimulation begins with strength of $\tau = 0.8 \text{ dyne/cm}^2$ and $\tau = 8.0 \text{ dyne/cm}^2$ at 0.5 sec and its duration is 60 sec. In fig. 2a, Ca_{dc} starts to decline because IP_3 is generated after the shear stress stimulation. The minimum values are at about 1.73 mM for $\tau = 0.8$ and at 1.75 mM for $\tau = 8.0$. But the time to reach minimum value in $\tau = 8.0$ is shorter than the case of $\tau = 0.8$. After the minimum value is reached, both of the two curves increases with some low gradient. Fig. 2b presents the release of Ca^{2+} in the cytosol of the VEC. The maximum value of 150 nM is reached at about 18 sec after there occurs stimulation with shear stress of $\tau = 8.0$. In case of $\tau = 0.8$, the maximum value is about 138 nM at 21 sec after the stimulation starts. This results show small disparity with Wong *et al.*⁸'s data, perhaps due to some difference in parameter and constant values. However, they show qualitatively very similar results. Fig. 3 presents in normalized value the synthesis or release of endothelium-derived relaxing factor(EDRF) and prostacyclin(PGI_2). Qualitative agreement with the results of Wong *et al.*⁷ is obtained. However, it must be

recalled that in the work of Wong *et al.*⁷ the first trigger to production of EDRF and PGI_2 is not by shear stress but by some agonists like bradykinin. The synthesis of EDRF and prostacyclin depends on the release of IP_3 and Ca_i . Therefore the model for EDRF and PGI_2 release used in Wong *et al.*⁷ is also useful in the present study. In the case of $\tau = 8.0$ the curve shows a larger and faster maximum value compared to the case of $\tau = 0.8$.

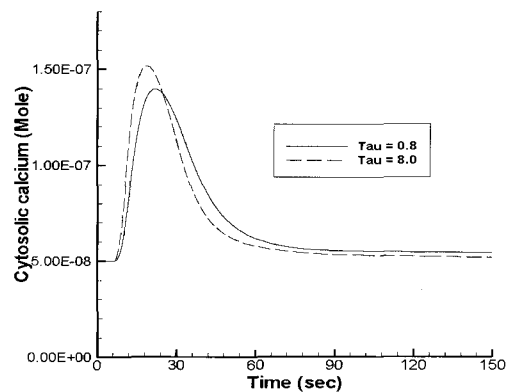
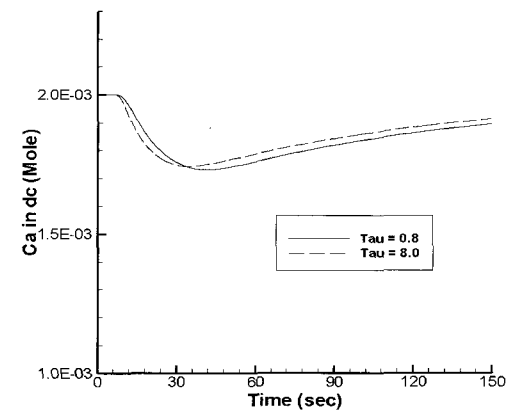
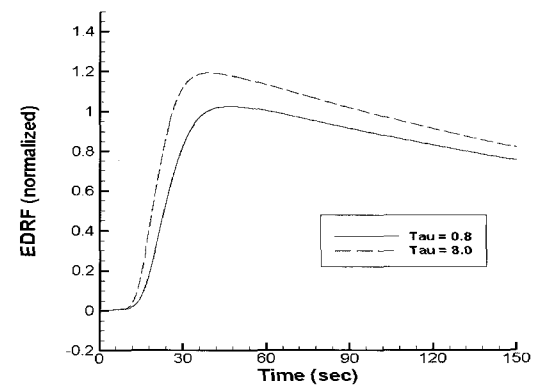


Fig 2. The time history of Ca^{2+} in the dc(a); that of intracellular Ca^{2+} concentration induced by constant shear stress(b).



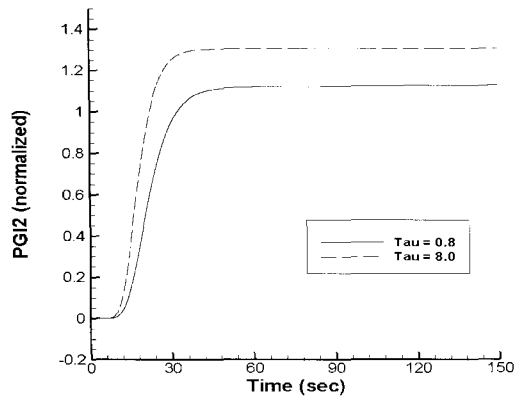


Fig 3. The time history of release or synthesis of EDRF(a); prostacyclin induced by constant shear stress(b).

Effect of repetitive shear stress

The effect of repetitive shear stress is tested under the same condition as Wong *et al.*⁸. As one can observe from fig. 4a, shear stress of duration 60 sec and strength $\tau = 1.6 \text{ dyne/cm}^2$ is repetitively applied with time interval of 120 sec. The Ca_{dc} is depleted during the stimulation, but is recovered in the interval time between stimuli. So we see the gradual and cyclic change of Ca^{2+} in dc, and even the amplitude of change is getting reduced; see fig. 4b. In fig. 4c, The Ca_i transient decrease with subsequent stimuli and this is similar to the Ca_i reported by Shen *et al.*³. The peak Ca_i values in the curve are sequentially 147 nM , 117 nM , 88 nM and 77 nM . This attenuation of Ca_i is caused by a decrease of $P[IP_3]$ due to inhibition by Ca_i of the production of IP_3 . One can check the decrease of $P[IP_3]$ from fig. 4f. EDRF and prostacyclin releases are presented in fig. 4d. EDRF release moves like a series of waves in which the peaks are getting reduced. This would be caused by the same reason as we discussed the attenuation of Ca_i or the transient peak values. Prostacyclin generation increases like a step but the interval between two adjacent jumps is getting shorter. This also is explained by the attenuation phenomena.

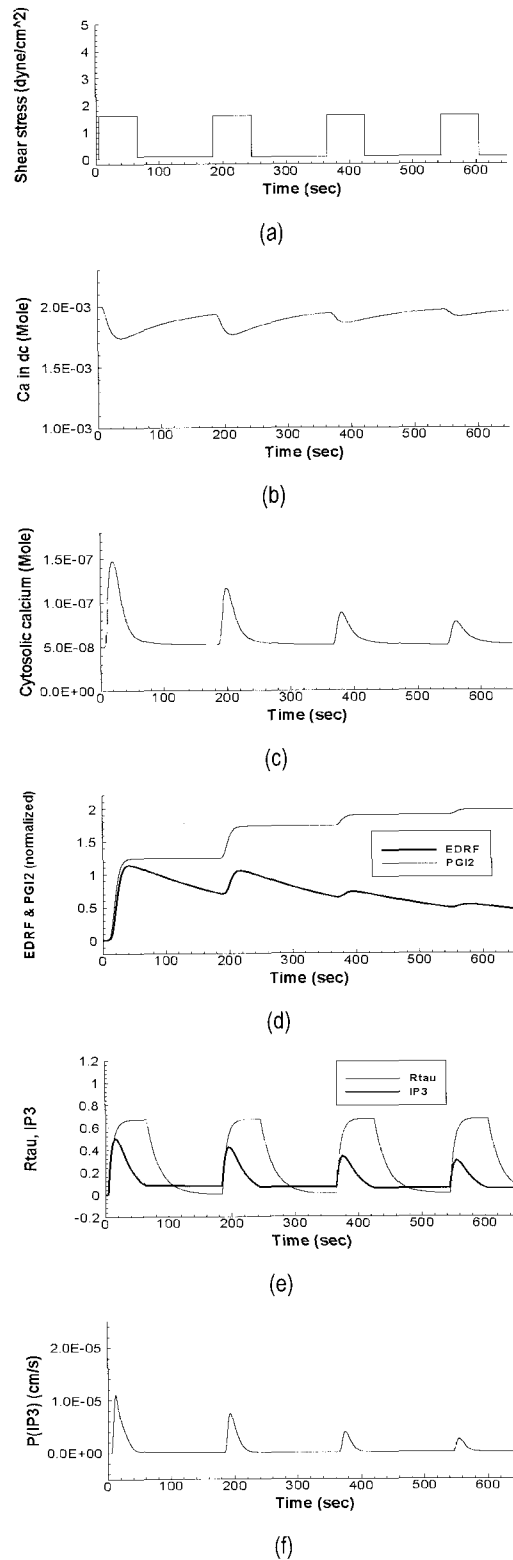


Fig 4. The time history of shear stress(a); Ca^{2+} in the dc(b); intracellular Ca^{2+} concentration change(c); EDRF & prostacyclin synthesis(d); deformation rate of mechanoreceptor and release of IP_3 (e); permeability of dc induced by repetitive shear stress(f).

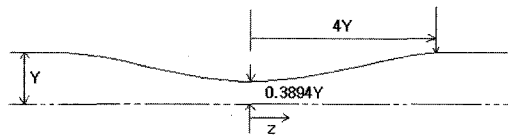


Fig 5. The geometry of an angiostenosis.

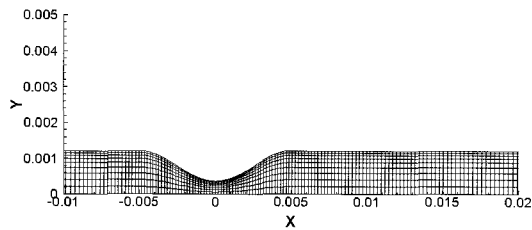


Fig 6. Computational grid in an angiostenosis (2D symmetric).

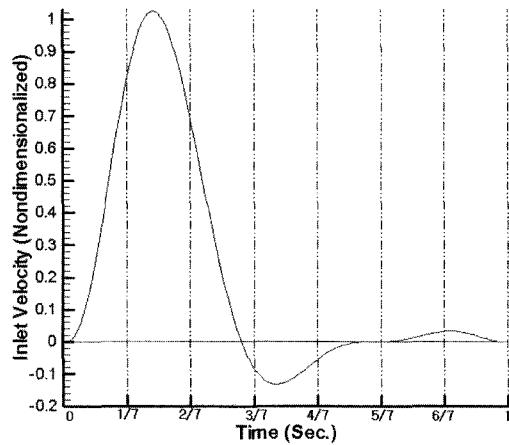


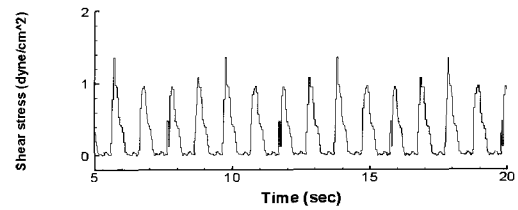
Fig 7. Physiological pulsatile blood flow condition at the inlet. Velocity is normalized by its maximum and period is 1 sec.

Effect of shear stress obtained by CFD

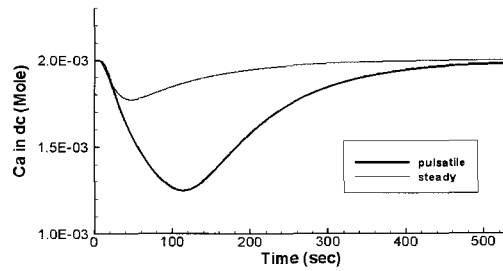
the possible shear stress variation in human artery or vein, we first calculate two-dimensional case. The geometry of the vessel has inlet height of $Y = 2.5 \text{ mm}$ and the occlusion shape is same as that of Bluestein¹⁰, namely,

$$y = Y + 0.3053Y \left[1 + \cos\left(\frac{\pi z}{4Y}\right) \right] \quad (10)$$

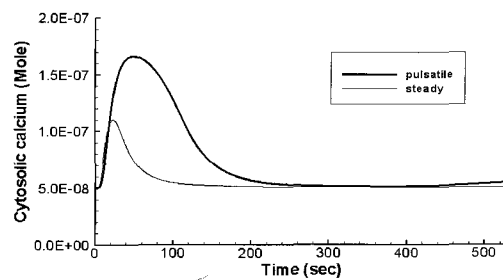
With this shape of the occlusion, patency is 39% at the narrowest place of the stenosed channel; see fig.5. The computational grid based on this geometry is in fig. 6



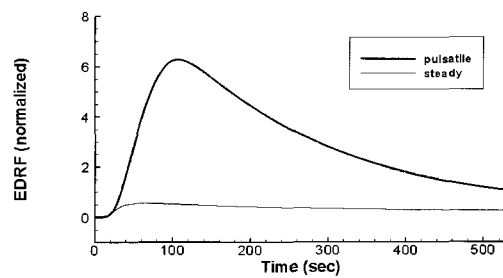
(a)



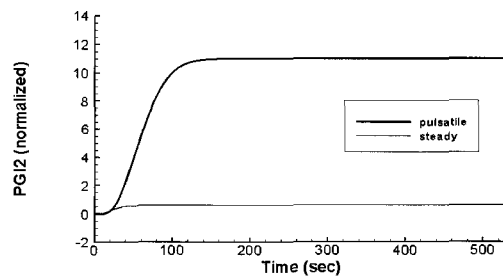
(b)



(c)



(d)



(e)

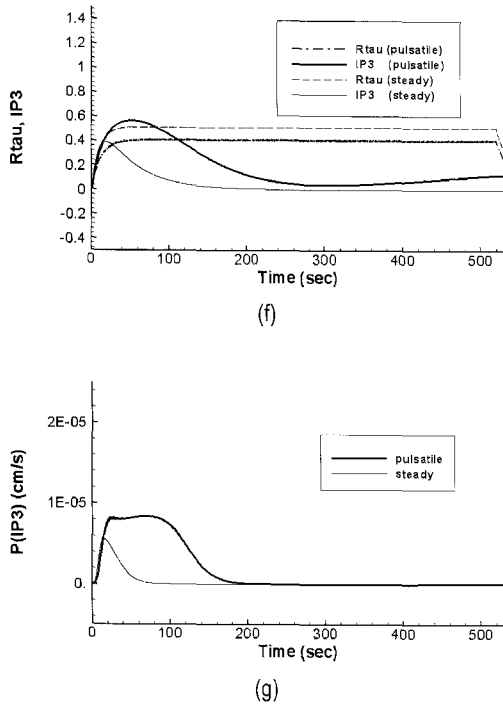


Fig 8. The time history of shear stress (a); Ca^{2+} in the dc(b); intracellular Ca^{2+} concentration change(c); EDRF & prostacyclin synthesis(d,e); deformation rate of mechanoreceptor and release of IP_3 (f); permeability of dc(g) induced by shear stress. The data are from CFD and hold true at a specific location(5Y to the right from the narrowest point of the stenosis).

Inlet conditions are given by reproducing some physiological blood flow data. Here the Reynolds number is 360 with peak velocity 36 cm/s and the half inlet width, $Y = 2.5 \text{ mm}$. Fig. 7 shows the pulsatile inlet velocity having a period of one second. Its peak has unit value as it is normalized by the maximum velocity.

After the computation, we get spatially and temporal distribution of wall shear stress. In particular, we pay attention to a location just after the stenosis. Fig. 8a represents the time history of wall shear stress at the location 5Y right to the narrowest point of stenosis. In this area the blood flow is separated from the wall and makes recirculation so that the time-averaged shear stress falls lower than that at the non-stenosed location. Therefore this area is important in hemodynamic view point in order to investigate the thrombogenesis or the origin of atherosclerosis. In fig. 8a, all the shear stress data are in their absolute value; the peak value is

1.3575 dyne/cm^2 and the time-average value is

0.3114 dyne/cm^2 .

With this time history of the wall shear stress, we now apply the vascular endothelial cell model. To make a comparison, the result obtained by a time-averaged steady shear stress stimulation ($\tau = 0.3114 \text{ dyne/cm}^2$)

is also shown in fig. 8. Pulsatile shear stress induces much faster depletion of Ca^{2+} from the deep compartment (dc). The minimum value of Ca_{dc} in the physiological pulsatile shear case is around 1.25 mM which is three times higher amount of depletion than the steady shear case; see fig. 8b. In fig. 8c, Ca_i transient shows the same tendency. Steady shear stress elicits a maximum value of $Ca_i = 110 \text{ nM}$ but the physiological pulsatile shear stress elicits a maximum value of $Ca_i = 165 \text{ nM}$. That is 115 nM above the resting level

$Ca_{i,0} = 50 \text{ nM}$. In case of the steady shear stress stimulation, peak Ca_i value jumps 60 nM above the resting level. The physiological pulsatile shear stress case shows slower but higher response than the steady shear stress case. Fig. 8d and fig. 8e represents the release and synthesis of EDRF and prostacyclin. They show that the physiological pulsatile shear stress induces release of EDRF and prostacyclin in higher amount than the steady shear stress case. Moreover the peak value of EDRF is as much as 13 times higher in the case of physiological pulsatile shear stress than the steady shear stress case. Prostacyclin production is also different between the physiological pulsatile shear stress and the steady shear stress. Its peak value is almost 44 times higher in the case of physiological pulsatile shear stress than the steady shear stress. The production of IP_3 in the physiological pulsatile shear case is higher and it decreases more slowly than the case of steady shear stress; see fig. 8f. Finally, the permeability of the dc ($P[IP_3]$) remains higher and longer in the physiological pulsatile shear stress; see fig. 8g.

Discussion

The calcium dynamics of vascular endothelial cells modulated by the physiological shear stress is simulated. Change in calcium concentration, and EDRF &

prostacyclin production are reproduced for the physiologically pulsating flow having periodic shear stress. The present results show for the steady flow case qualitatively similar result as Wong *et al.*⁸. However, the results of two steady cases were not exactly same because there was some difference in parameters, constant values and equations used for numerical simulation. For example, Wong *et al.*⁸ did not solve all the differential equations but opted some analytical solutions instead.

In this study, we combined the cell model with the physiological shear stress information obtained by CFD technique. Pulsatile shear stress induced larger intracellular Ca^{2+} transient and much higher amount of EDRF and prostacyclin release than the case of steady shear stress. This results well agree with the observation that pulsatile flow is powerful for EDRF & prostacyclin production and imply that vascular endothelial cells are indeed sensitive to the rate of change of shear stress¹¹⁻¹⁴. With the time history of EDRF and prostacyclin release obtained from the present physiological shear stress case, activation of vasodilation may be now predicted.

Fig. 8 shows that after stimulation about 200 sec in the physiological pulsatile shear stress of 1Hz, the model cell becomes insensitive to further stimuli. This desensitization is not due to the depletion of intracellular

Ca^{2+} pool but because of $f(Ca_i)$ -dependent IP_3 inactivation) increasing almost up to 1. This increase of inactivation f reduces the release of IP_3 and at the same time decrease of intracellular Ca^{2+} concentration; see fig. 8g. During this period of desensitization, the dc(deep compartment) is refilled by the Ca^{2+} from the sc(surface compartment). Then the VEC which is insensitive to further shear stress stimuli remain responsive to chemical stimulation of ATP and produce a large decrease in intracellular Ca^{2+} concentration³.

Early in the development of coronary atherosclerosis during hypercholesterolemia in humans, endothelium dependent responses were impaired by a depressed receptor-mediated initiation of the synthesis of EDRF whereas flow-dependent dilation was well preserved¹⁵. However, as the atherosclerosis is more advanced and the angiostenosis deforms the lumen of the blood vessel, the flow-induced vasodilation was also abolished¹⁵. The present study shows that even behind the stenosis the pulsatility of flow and shear stress is not lost and EDRF

& prostacyclin are still synthesized. Although the flow-induced vasodilation is continued, the impaired endothelial function to agonists such as acetylcholine or bradykinin would decline the whole responsiveness of endothelial cell vasodilation. Furthermore, the amplitude of pulsatile shear stress is remarkably reduced in a separated recirculating flow behind the vascular stenosis. It would result in diminished synthesis or release of EDRF & prostacyclin.

This low shear stress in the stenosed vessel raises many problems to human circulatory function. The distribution of the recirculation zone depends on the type and shape of developing atherosclerosis. Intensive investigation on the endothelial cell response in the recirculation zone is desired. We are making progress on this topic now.

In summary, we simulated by CFD technique the effect of the physiological pulsatile shear stress on the stenosed human blood vessel. The shear stress is allowed to stimulate the model VEC to trigger calcium dynamics modulation and release of EDRF & prostacyclin. We concluded that pulsatility of shear stress kept the vasodilation function in the stenosed blood vessel. We plan to investigate in the future about the vascular endothelial cell function in the whole recirculation zone behind a stenosis.

References

1. Ando J, Komatsuda T, Kamiya A, Cytoplasmic calcium response to fluid shear stress in cultured vascular endothelial cell. *In Vitro Cell Dev. Biol.* 1988;24:871-877
2. Nollert MV, Eskin SG, McIntire LV, Shear stress increases inositol triphosphate levels in human endothelial cells. *Biochim. Biophys. Res. Commun.* 1990;170:281-287
3. Shen J, Lusinskas FW, Connolly A, Dewey CF Jr., Gimbrone MA, Fluid shear stress modulates cytosolic free calcium in vascular endothelial cells. *Am. J. Physio.* 1992;262:C384-C390
4. Ando J, Ohtsuka A, Kawamura T, Kimiya A, Wall shear stress rather than shear rate regulates cytoplasmic Ca^{2+} responses to flow in vascular endothelial cells. *Bio-chem. Biophys. Res. Commun.* 1993;190:716-723

5. Olesen SP, Clapham DE, Davies PF, Hemodynamic shear stress activates a K^+ current in vascular endothelial cells. *Nature* 1988;311:168-170
6. Kuo L, Davies MJ, Chilian WM, endothelium-dependent, flow-induced dilation of isolated coronary arteries. *Am J. Physiol.* 1990;259:H1063-H1070
7. Wong AYK, Klassen GA, A model of cytosolic calcium regulation and autacoids production in vascular endothelial cell. *Basic Res. Cardiol.* 1992;87:317-332
8. Wong AYK, Klassen GA, A model of Electrical activity and cytosolic calcium dynamics in vascular endothelial cells in response to fluid shear stress. *Annals of Biomedical Engineering* 1995;23:822-832
9. Sanchez-Bueno A, Dixon CJ, Woods NW, Cuthbertson KSR, Cobbold PH, Inhibitors of protein kinase C prolong the falling phase of each free-Ca transient in a hormone-stimulated hepatocyte. *Biochem. J.* 1990;268:627-632
10. Bluestein D. et al. Vortex shedding in steady flow through a model of an arterial stenosis and its relevance to mural platelet deposition. *Annals of Biomedical Engineering* 1999;27:763-773
11. Frangos JA, Eskin SG, McIntire LV, Ives CL, Flow effect on prostacyclin production by cultured human endothelial cells. *Science Wash. D.C.* 1985;227:1477-1479
12. Hutchesson IR, Griffith TM, Release of endothelium-derived relaxing factor is modulated by frequency and amplitude of pulsatile flow. *Am. J. Physio.* 1991;261:H257-262
13. Pohl UR, Busse E Kuo, Bassenge E, Pulsatile perfusion stimulates the release of endothelial autacoids. *J. Appl. Cardiol.* 1986;1:215-235
14. Rubanyi GM, Romero JC, Vanhoutte PM, Flow-induced release of endothelium-derived relaxing factor. *Am. J. Physiol.* 1986;250:H1145-H1149
15. Zeiher AM, Drexler H, Wollschlager H, Just H, Modulation of coronary vasomotor tone. Progressive endothelial dysfunction with different early stages of coronary atherosclerosis. *Circulation* 1991;83:391-401